

# Comparison of Optical Emission Spectrometric Measurements of the Concentration and Energy of Species in Low-pressure Microwave and Radiofrequency Plasma Sources\*

Jürgen Röpcke, Andreas Ohl and Martin Schmidt

*Institute for Low-Temperature Plasma Physics, Robert-Blum-Str. 8–10, D-17489 Greifswald, Germany*

Understanding of specific plasmachemical reactions occurring in plasma sources with the addition of complicated molecules requires knowledge of the particular plasma conditions. The subject of the present paper is a comparison of the spectrometrically measured relative concentration distributions and energies of species in low-pressure argon discharges containing an organosilicon compound, hexamethyldisiloxane (HMDSO), which has a large molecular size. The optical diagnostics were performed with three different plasma sources: a special planar microwave plasma source ( $\nu=2.45$  GHz), an r.f. planar reactor ( $\nu=13.56$  MHz) and a capacitively coupled r.f. model discharge tube ( $\nu=460$  kHz). The energy distribution functions of each plasma are not the same, but their general forms are similar to a Maxwell–Boltzmann distribution. The results of comprehensive, spatially resolved measurements of the relative concentrations of atoms and radicals (H, Si, CH and C<sub>2</sub>), the neutral species gas temperature, rotational temperature and optical excitation temperature are reported. The use of the same gas mixture in three plasma sources, each of distinct construction, excited by different frequencies, once again clearly indicates that the comparison and interpretation of optical diagnostic results has to be done very carefully, taking into consideration the discharge conditions. Results obtained by actinometry show considerably different particle density gradients in the plasmas. Gradients of the excitation temperatures ( $T_{\text{exc}}=0.45\text{--}0.7$  eV) are less, but the neutral gas temperatures also exhibit large spatial gradients ( $T_g$  = ambient temperature, about 2000 K). This clearly indicates the absolute necessity of spatially resolved optical emission measurements for the purpose of comparisons between different plasma sources.

**Keywords:** *Optical emission spectrometry; plasma diagnostics and characterization; low-pressure microwave and r.f. discharges; species concentration and energy*

The parameter set needed to describe the properties of non-equilibrium, low-pressure gas discharge plasmas is very large. Owing to specific excitation mechanisms many different particle ensembles exist. Since energy is transferred step by step from the external electric field to plasma electrons and plasma ions, and then to activated neutral species, and as the transfer efficiencies of these processes differ by orders of magnitude, particle ensembles with different thermodynamic properties exist simultaneously. The energy of single particles of each of these ensembles is distributed within a certain characteristic range. Normally, the energy distribution functions are not equal to each other but their general form is similar to a Maxwell–Boltzmann distribution. Therefore, following thermodynamic methods, each of these particle ensembles can be characterized by generalized thermodynamic variables, such as temperature and the number densities of the particles. In this way, it is possible, as a first approach, to describe the properties of low-pressure, non-equilibrium plasmas by a set of temperatures and number densities. When considering systematic investigations of the fundamental properties and application of plasmas, knowledge of this set of parameters must be available. As the largest differences exist between the electron ensemble on one side and all other, heavier particle ensembles on the other side, the parameter set can be reduced to two ensembles in the simplest case. The heavy particle ensemble includes ions as well as radicals and non-activated neutral species. If, as is usual, the degree of ionization is low, this heavy particle ensemble can be described by the properties of the neutral species. This two-temperature model is the simplest approach to characterize low-pressure, non-equilibrium plasmas, and is well established in the characterization of pure rare gas discharges.

The addition of molecules, especially of complex molecules, to rare gas discharges leads to an enormous increase of the number of species ensembles. Nevertheless, the differences between electrons and neutral species remain high. Hence, the characterization of these plasmas can also begin with the determination of electron temperature, neutral species gas temperature and densities of the most relevant species. However, many of these molecular gas plasmas, which are very relevant in practical applications, are chemically active. Under these circumstances a complex investigation of plasmas including probe measurements, mass spectrometry and optical methods, is difficult, and measuring methods which do not disturb the plasma become very important. Optical emission spectrometry (OES) is one of these methods of measurement. It can detect a certain number of different species and the determination of characteristic temperatures is also possible.

The subject of the present paper is OES measurements in low-pressure argon discharges containing small additions of an organosilicon compound, hexamethyldisiloxane (HMDSO). In some cases the carrier gas also contains a few per cent of helium or nitrogen for measuring purposes. Three different plasma sources are compared: a special planar microwave plasma source ( $\nu=2.45$  GHz), an r.f. planar reactor ( $\nu=13.56$  MHz) and a capacitively coupled r.f. model discharge tube ( $\nu=460$  kHz). The results concerning the spatial distribution of hydrogen and silicon atoms and of CH and C<sub>2</sub> radicals, neutral species gas temperature, rotational temperature and optical excitation temperature, which is closely related to the energy of the electron gas, are reported. Knowledge of these parameters is vital for the detailed analysis of the plasmachemical activity of these plasmas, which results in the growth of so called plasma polymer films on the plasma vessel walls and on the electrodes. Although it is known, especially with plasmopolymerization of HMDSO, that large differences between processes in r.f. excited plasmas and microwave

\* Presented in part at the 1993 Winter Conference on Plasma Spectrochemistry, Granada, Spain, January 10–15, 1993.

plasmas exist,<sup>1</sup> the microphysical explanation of these differences is still a matter of discussion. The latter is a result of the complex character of these plasmas. Hence, a complex comparison of these would be interesting.

The analysis of the emission measurements includes a number of assumptions, which are described as follows.

As a matter of principle, it is assumed that the Corona model is valid, describing the emission of spectral lines or molecular bands corresponding to the population of excited states, as determined by the balance between collisional excitation and spontaneous radiative decay only. The validity of this assumption is mainly based on the low degree of ionization in these plasmas, which is a maximum of  $1 \times 10^{-4}$  in all cases.

If the population of the excited atomic states corresponds to a Boltzmann distribution, the so called electronic excitation temperature or excitation temperature  $T_{\text{exc}}$  of the emitting atoms can be derived by means of relative line intensity measurements. In this case the value  $\log(I\lambda/gA)$  is a linear function of the excitation energy. Using the Boltzmann plot method and plotting  $\log(I\lambda/gA)$  as a dependent of the excitation energy, the slope of the plot is related to the excitation temperature. It is equal to  $-0.625/T_{\text{exc}}$  when  $E$  is in  $\text{cm}^{-1}$ ,  $I$  is the line intensity,  $\lambda$  the line wavelength,  $A$  the transition probability and  $g = g_k/g_j$  is the quotient of the statistical weights of the two atomic levels ( $k > j$ ). In the present paper the excitation temperature is measured by using the argon line intensities. The reason for the use of argon lines is the existence of a large number of good detectable lines in the spectral range available. The transition probabilities were taken from the literature.<sup>2</sup> In this instance the argon lines with wavelengths 603.2 nm (transition probability  $A = 0.246 \times 10^8 \text{ s}^{-1}$ ), 614.5 nm ( $A = 0.079 \times 10^8 \text{ s}^{-1}$ ), 667.7 nm ( $A = 0.0241 \times 10^8 \text{ s}^{-1}$ ) and 696.5 nm ( $A = 0.674 \times 10^8 \text{ s}^{-1}$ ) were used.

The spatially resolved relative concentrations of atoms and molecules are determined by actinometry. This method compares the emission of the species of interest with the emission of, for example, an inert gas, the so called actinomer, which is added in small amounts to the discharge gas mixture.<sup>3</sup> The preconditions ensuring validity of actinometric results are as follows. The addition of the actinomer should not essentially influence the discharge characteristics, the electron energy distribution has to be spatially constant and the emitting states are solely excited by electron impact upon the ground state. The last condition means that dissociative excitation should be negligible.

Often these preconditions are not completely fulfilled, therefore the plasmas under investigation are always checked for changes of electron energy distribution. For this purpose the intensity ratio of the  $\text{H}\alpha$  to the  $\text{H}\beta$  line is assumed to be a useful measure of relative changes, as has been done previously.<sup>4</sup>

For the determination of translational or kinetic temperature of heavy particles from Doppler broadening of spectral lines, the velocity distribution of these particles is assumed to be Maxwellian. This is self-evident, since spectral linewidth measurements are only performed for neutral species, and since the degree of ionization of the plasmas is low, the kinetic temperature is assumed to agree with the neutral gas temperature. The influence of microfield Stark effect is neglected owing to low absolute electron densities, not exceeding  $1 \times 10^{-12} \text{ cm}^{-3}$ . Because in most cases natural linewidths also can be negligible, the line profile is pure Gaussian. The full width of half maximum (FWHM) of the Gaussian profile directly represents the Doppler broadening:

$$\lambda_d = (8 \times \ln 2 \times k/mc^2)^{1/2} \times T_g^{1/2} \times T_g^{1/2} \times \lambda_m$$

where  $T_g$  = neutral gas temperature (K);  $m$  = particle mass

(kg);  $\lambda_m$  = wavelength (nm) in the middle of the profile;  $k$  = the Boltzmann constant; and  $c$  = the velocity of light ( $\text{m s}^{-1}$ ).<sup>5</sup>

The  $\text{H}\alpha$  line is an extensively studied spectral line. Owing to the fine structure splitting it consists of seven closely related components. The relative intensities are found to depend on the discharge conditions. At neutral species gas temperatures lower than about 600 K, this fine structure line splitting must be taken into account by deconvolution. In this temperature region the  $\text{H}\alpha$  line appears as a doublet, each component being a blend of different fine structure lines. An experimental separation of the two main components of 0.014 nm, which only requires a relatively low instrumental error of about  $1 \times 10^{-3} \text{ nm}$ , is sufficient for determination of the neutral species gas temperature.

Another method for the determination of the gas temperature used in this work is the measurement of the rotational intensity distribution of excited molecular bands. In order to use this method, close correspondence of the rotational state population to the gas temperature must be assumed. The energy separation between the rotational levels of the measured molecules is very small. This makes the rotational excitation *via* interaction with the translation degrees of freedom of the molecules very efficient. Excitation by electron collisions or other processes, which can result in non-Boltzmann distributions of the excited rotational levels, is therefore neglected.

The rotational temperature is derived by measuring the relative intensities of rotational lines within a vibrational band. It is assumed that all rotational lines in the vibrational band have the same transition probability. The sensitivity of the apparatus is taken into account. Under these conditions the following relationship can be written:

$$\begin{aligned} \log(I/p) &= \text{const} - [p(p \pm 1)B_v/hc]/2.3026kT_{\text{rot}} \\ &+ = \text{R-branch} \\ &- = \text{P-branch} \end{aligned}$$

where  $T_{\text{rot}}$  is the rotational temperature,  $B_v$  the rotational constant of the upper electronic level,  $I$  the rotational line intensity,  $p$  is the rotational quantum number and  $k$  the Boltzmann constant. In a Boltzmann plot diagram  $\log(I/p) = f[p(p \pm 1)]$  the slope of the straight line gives the rotational temperature.

In this paper results of rotational temperature measurements made by means of nitrogen molecule emission are reported. A small amount of nitrogen is added to the plasma. When considering the nitrogen emission, the molecular band of the second positive system  $\text{C}^3\Pi_u(0) \rightarrow \text{B}^3\Pi_g(0)$  with its bandhead at 337.1 nm is used. To minimize the influence of branch overlapping, the R-branch rotational line distribution from quantum numbers greater than 20 is measured. For these large quantum numbers the rotational lines were clearly identified. In this case the deviations from the linear relationship in the Boltzmann plot were less than 5%.

## Experimental

The measurements were performed using a special planar microwave plasma source ( $\nu = 2.45 \text{ GHz}$ ), a capacitively coupled r.f. model discharge tube ( $\nu = 460 \text{ kHz}$ ) and an r.f. planar reactor ( $\nu = 13.56 \text{ MHz}$ ). In each case argon was used as the carrier gas. Hexamethyldisiloxane was added in concentrations of 0.2–10%.

The optical diagnostic system, a schematic diagram of which is shown in Fig. 1, in combination with the microwave plasma source, consists of a computer controlled 2 m grating spectrometer and a high sensitivity optical multichannel analyser system, OMA-VISION (PAR).

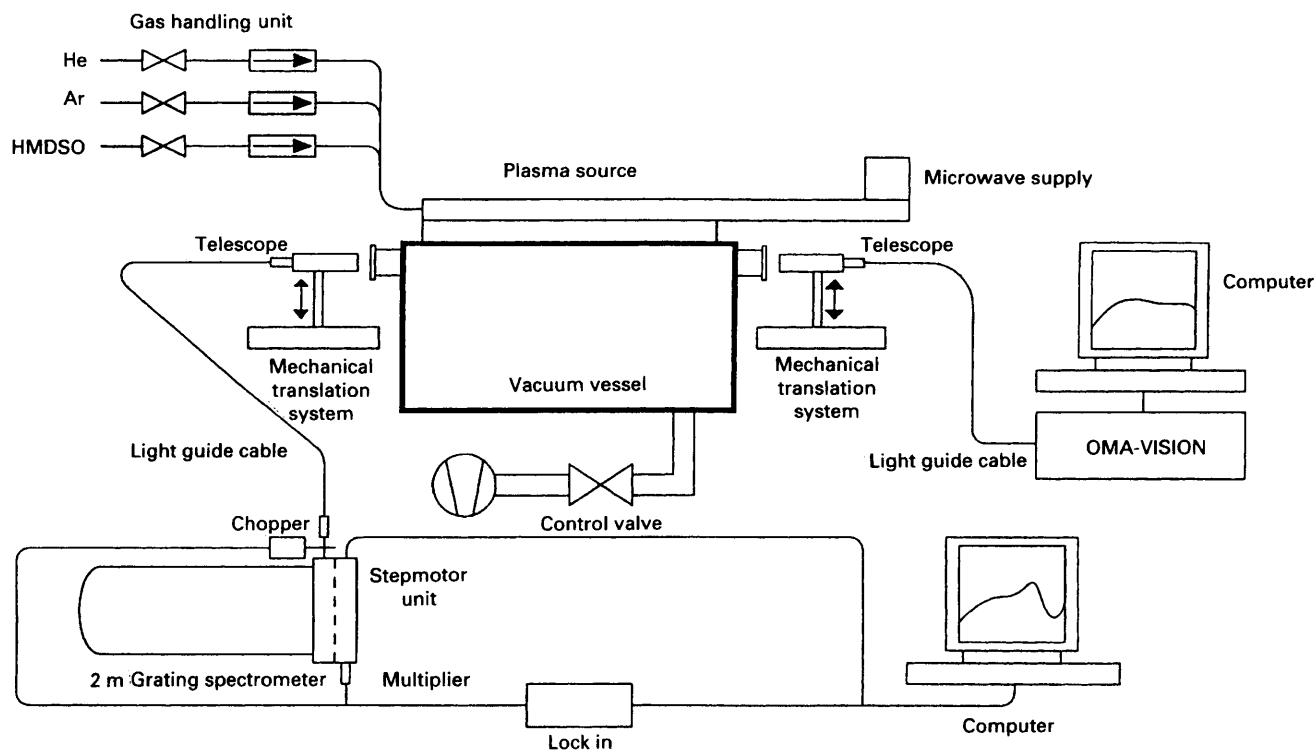


Fig. 1 Schematic diagram of the experimental set-up including the planar microwave plasma source

The 2 m grating spectrometer with quartz collimation optics and a grating with  $1302 \text{ grooves mm}^{-1}$  achieves a wavelength resolution of about  $1 \times 10^{-3} \text{ nm}$ . This allows Doppler line broadening measurements of the red  $H\alpha$  line for determination of neutral species gas temperature in the plasma down to ambient temperature. With respect to the plasma conditions, which are characterized by a variety of low intensity atomic lines and molecular bands and by relatively high noise levels, lock-in signal detection is used. The computer controlled data collection system used allows further treatment of the stored spectra. Fit and deconvolution procedures are very important, but smoothing, spreading out or averaging procedures were also used.

The OMA-VISION system is equipped with a 0.5 m grating monochromator and a Peltier cooled highly sensitive UV intensified charge coupled device (CCD) matrix detector. The maximum sensitivity of this detector is 4–10 photons per count. This system is used for

molecular band analysis for determination of the rotational temperature and for atomic line intensity measurements. Molecular rotational band analysis is performed using a grating with  $2400 \text{ grooves mm}^{-1}$ . This provides a wavelength resolution of about 0.1 nm, which is sufficient for most cases. Atomic line intensities were measured using a grating with  $600 \text{ grooves mm}^{-1}$ . For spatially resolved measurements, a quartz telescope and a rectangular slit-like aperture are mounted on a mechanical translation system combined with a quartz light guide cable used for light transfer to the monochromators.

The planar microwave plasma source investigated works on the principle of distributed coupling of microwave power into the vacuum vessel. In this way the difficulties concerning the generation of large area microwave plasmas are overcome, which arise mainly because of the short wavelength of microwaves and their low penetration depth into the plasma. For a more detailed description of this type of microwave plasma source see ref. 6.

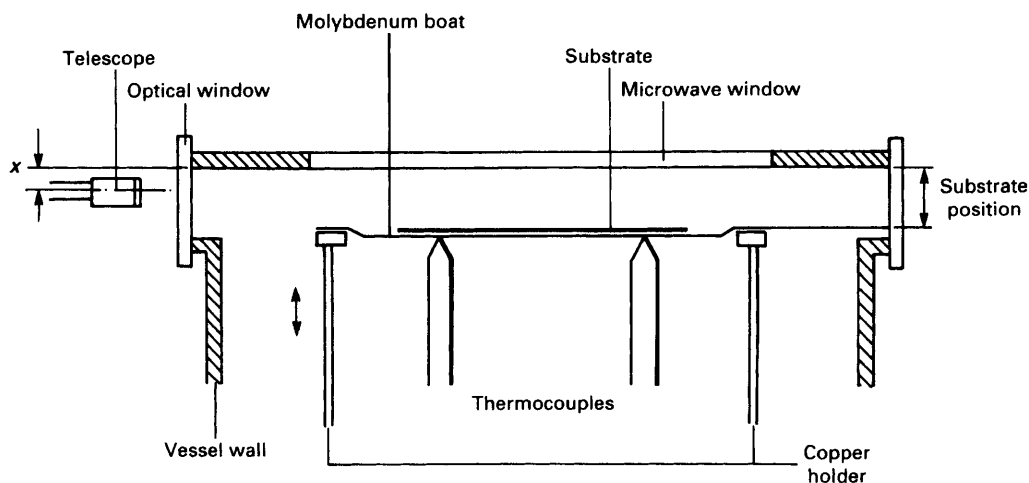


Fig. 2 Details of the plasma region and substrate arrangement ( $x$ , distance to the microwave window)

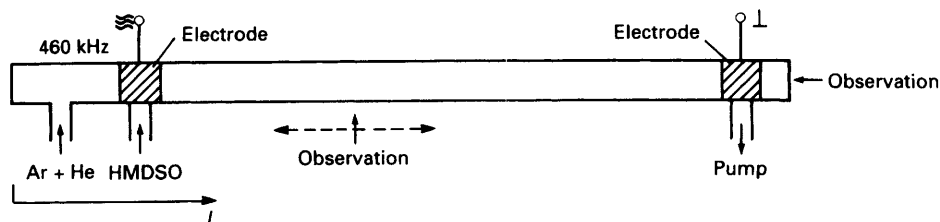


Fig. 3 Schematic diagram of the r.f. model discharge tube ( $l$ , side-on observation position)

The test source used generates a long, extended, laterally homogeneous, planar plasma for low-pressure plasma processing with lateral dimensions of  $14 \times 4$  cm. Sources with up to  $50 \times 10$  cm lateral dimensions have been achieved. In Fig. 2 details of the microwave plasma region and substrate arrangement are shown. The microwaves which penetrate into the reaction vessel through the quartz microwave window are strongly absorbed. Therefore, the plasma is strongly decaying in the direction normal to the window. The thickness of the active microwave power absorbing plasma region, with electron densities above the so called cut-off density of about  $7 \times 10^{10} \text{ cm}^{-3}$ , does not exceed a few centimeters at low pressures, and increasing the pressure compresses this region. The active plasma region is followed by another decaying, diffusive afterglow plasma region. Usually, the extended planar substrates for plasma polymerization are placed in this afterglow region.

The optical emission of optically thin plasmas was spatially resolved, being observed in an end-on configuration by means of a special quartz telescope, resulting in laterally integrated information. Plasma homogeneity along the line of sight was ensured. Therefore, margin effects of the plasma edge regions, which significantly influence linewidth measurements, can be neglected.

Fig. 3 shows a schematic diagram of the r.f. model discharge tube used. To ensure well defined, stable discharge conditions a gas flow regime with a separate supply

of the monomer downstream of the argon supply is necessary. The r.f. energy ( $\nu = 460 \text{ kHz}$ ) with maximum 40 W power is capacitively coupled to the plasma. The over-all discharge volume is about  $50 \text{ cm}^3$ . In addition to the end-on observation, side-on observation of the spectral emission is also possible.

The 13.56 MHz r.f. planar reactor is of the usual type. It consists of two circular electrodes, one of which is grounded and the other powered by capacitive coupling. Both electrodes have the same diameter of 13 cm. The distance between the electrodes is 4 cm. The r.f. power is supplied via a matching network. The optical emission is observed side on. Additionally, Langmuir probe and mass spectrometry measurements are possible. The gas supply is organized in a flow regime using a flow controller gas inlet system.

### Results and Discussion

In Fig. 4(a) measurements of the relative spatial concentration distributions of Si atoms, H atoms, CH radicals and  $\text{C}_2$  radicals between the microwave quartz window and the substrate in the microwave plasma source are shown with addition of 0.2% HMDSO. The species exhibit pronounced local concentration maxima, which are shifted toward the active plasma region near the window. Under these discharge conditions, atomic line emission of the helium actinometer is undetectable, hence an argon line (750.4 nm) is used for actinometric estimation. The low helium emission is believed to be due to the relatively low electron temperature. In contrast, between the electrodes of the r.f.

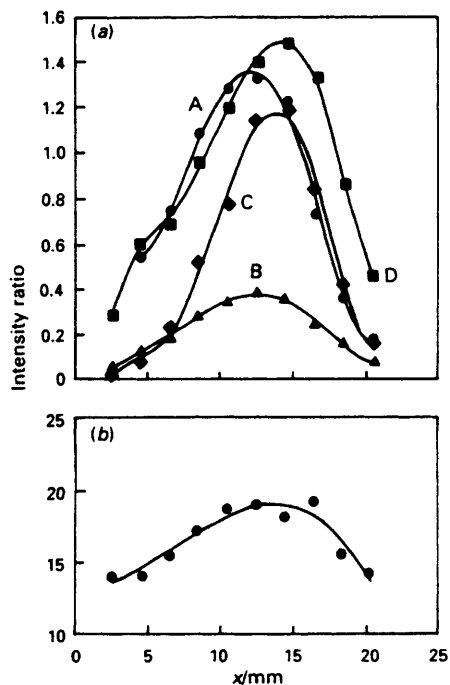


Fig. 4 (a) Dependence of the intensity ratios: A,  $\text{C}_2$  516 nm system:Ar 750.4 nm; B, CH 430 nm system:Ar 750.4 nm; C, Si 288.2 nm:Ar 750.4 nm; and D, H $\alpha$ :Ar 750.4 nm ( $\times 10$ ) on the distance to the microwave window. (b) Dependence of the intensity ratio H $\alpha$ :H $\beta$  on the distance to the microwave window. Ar+0.2% HMDSO+2.5% He;  $p = 230 \text{ Pa}$ ; and substrate position,  $s = 25 \text{ mm}$

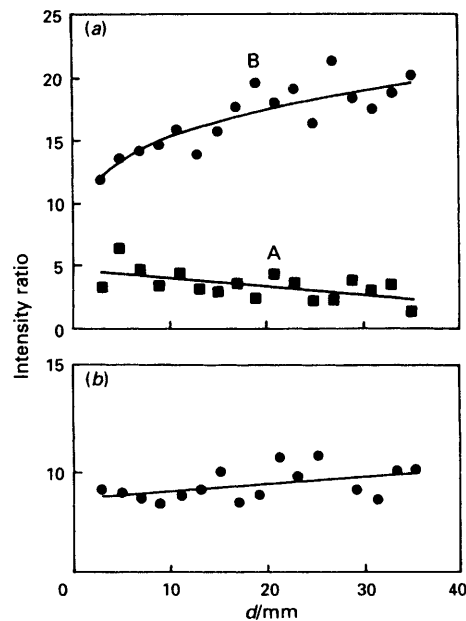
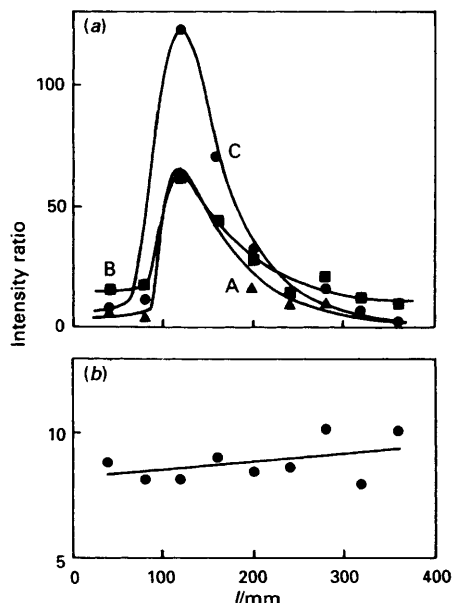


Fig. 5 (a) Dependence of the intensity ratio of A,  $\text{C}_2$  516 nm system:He 587.6 nm and B, CH 430 nm system:He 587.6 nm on the position between the electrodes,  $d$ , of the r.f. planar reactor. (b) Dependence of the intensity ratio H $\alpha$ :H $\beta$  on the position between the electrodes,  $d$ , of the r.f. planar reactor. Ar+10% HMDSO+5% He,  $p = 70 \text{ Pa}$ ,  $d = 0 \text{ mm}$  grounded electrode



**Fig. 6** (a) Dependence of the intensity ratio of: A, C<sub>2</sub> 516 nm system:He 587.6 nm ( $\times 10^{-2}$ ); B, CH 430 nm system:He 587.6 nm ( $\times 10^{-2}$ ); and C, Si 288.2 nm: He 587.6 nm on the side-on observation position,  $l$ , in the r.f. model discharge tube. (b) Dependence of the intensity ratio H $\alpha$ :H $\beta$  on the side-on observation position,  $l$ , in the r.f. model discharge tube Ar+10% HMDSO+2% He,  $p=70$  Pa

planar reactor such a concentration maximum of the CH and C<sub>2</sub> molecules is not observable [Fig. 5(a)].

In the r.f. model discharge tube, maxima of the relative Si, CH and C<sub>2</sub> concentrations appear directly downstream from the position where the HMDSO feed gas comes into the tube. For this discharge, spatial distributions of the polymer deposition rate were observed. The optical emission maxima [Fig. 6(a)] correlate with the spatial dependence of the deposition rate.

In all of the plasmas, the validity of actinometry was ensured. The ratios of the hydrogen line intensities indicate an almost constant electron temperature over the plasma region investigated [Figs. 4(b), 5(b) and 6(b)]. No order of magnitude changes were observed. One possible explanation for this effect is the relatively low level of HMDSO, resulting in an argon-hydrogen gas mixture of constant composition as the dominant plasma gas component over the entire discharge volume. The HMDSO is known to produce large amounts of atomic hydrogen under the influence of gas discharges. The ratio of H $\alpha$  to H $\beta$  in the microwave plasma source [Fig. 4(b)] is essentially higher

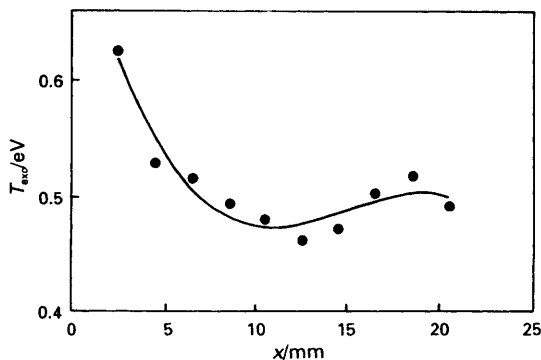


**Fig. 7** Dependence of the excitation temperature  $T_{exc}$  on the distance to the microwave window,  $x$ , (Ar+0.2% HMDSO;  $p=230$  Pa; substrate position:  $s=25$  mm, derived from argon line intensities)

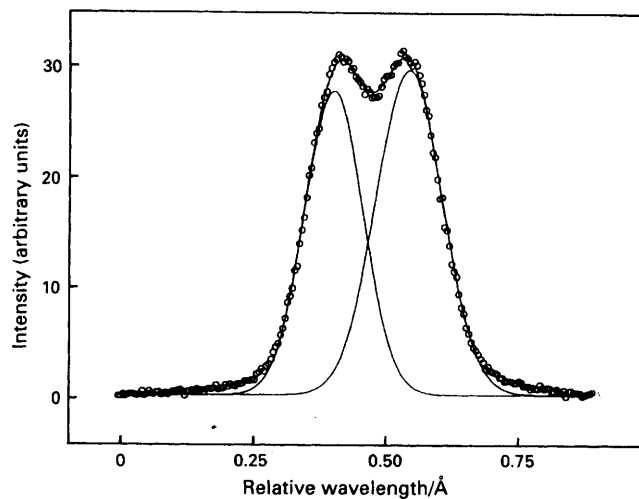


**Fig. 8** Experimental H $\alpha$  line profile fitted by Gaussian profiles

than in the r.f. plasma sources [Figs. 5(b) and 6(b)]. This indicates the expected lower electron energy of microwave plasmas. A certain flat maximum between the microwave window and the substrate must be recognized. In accordance to the H $\alpha$  to H $\beta$  intensity ratio, the spatial distribution of the excitation temperature  $T_{exc}$ , determined by argon line intensity relationships, shows a flat minimum between the microwave window and the substrate (Fig. 7). The tendency to decrease with increasing distance from the microwave window agrees well with former Langmuir probe measurements.<sup>7</sup> In the vicinity of the substrate the excitation temperature seems to be influenced by this additional wall.

In contrast to the excitation temperature, the neutral species gas temperature exhibits larger spatial variations.

In the r.f. model discharge tube, the neutral species gas temperature is derived from Doppler line broadening of the red H $\alpha$  line (656.3 nm) and rotational band analysis of the nitrogen molecule. The influence of fine structure line splitting on Doppler broadening is taken into account by using numerical fit procedures. This is recommended particularly in the medium temperature range exhibiting incomplete line splitting. So the error in temperature determination is reduced to 5–10%. Fig. 8 shows an example of such an experimental H $\alpha$  line profile fitted by Gaussian profiles. In Fig. 9 the dependence of the neutral species gas temperature,  $T_g$ , on the supplied power,  $P$ , is shown. The value of  $T_g$  increases slightly with increasing power. In contrast to this, the analysis of the nitrogen molecular emission resulted in rotational temperatures of

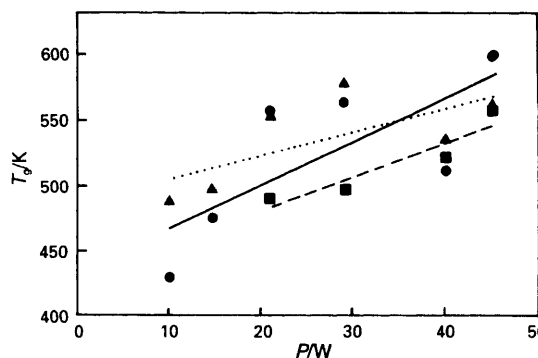


**Fig. 9** Dependence of the neutral gas temperature,  $T_g$ , on the power,  $P$ , in the r.f. model discharge tube (●, Ar 55 Pa; ▲, Ar 87 Pa; and ■, Ar+10% HMDSO 60 Pa, derived from H $\alpha$  Doppler line broadening)

# Explore Litigation Insights

Docket Alarm provides insights to develop a more informed litigation strategy and the peace of mind of knowing you're on top of things.

## Real-Time Litigation Alerts



Keep your litigation team up-to-date with **real-time alerts** and advanced team management tools built for the enterprise, all while greatly reducing PACER spend.

Our comprehensive service means we can handle Federal, State, and Administrative courts across the country.

## Advanced Docket Research



With over 230 million records, Docket Alarm's cloud-native docket research platform finds what other services can't. Coverage includes Federal, State, plus PTAB, TTAB, ITC and NLRB decisions, all in one place.

Identify arguments that have been successful in the past with full text, pinpoint searching. Link to case law cited within any court document via Fastcase.

## Analytics At Your Fingertips



Learn what happened the last time a particular judge, opposing counsel or company faced cases similar to yours.

Advanced out-of-the-box PTAB and TTAB analytics are always at your fingertips.

## API

Docket Alarm offers a powerful API (application programming interface) to developers that want to integrate case filings into their apps.

## LAW FIRMS

Build custom dashboards for your attorneys and clients with live data direct from the court.

Automate many repetitive legal tasks like conflict checks, document management, and marketing.

## FINANCIAL INSTITUTIONS

Litigation and bankruptcy checks for companies and debtors.

## E-DISCOVERY AND LEGAL VENDORS

Sync your system to PACER to automate legal marketing.